Theoretical study of the erbium-doped fiber laser passively mode-locked by nonlinear polarization rotation

M. Salhi, H. Leblond, and F. Sanchez
Laboratoire POMA, UMR 6136, Université d'Angers, 2 Boulevard Lavoisier, 49000 Angers, France
(Received 19 June 2002; published 9 January 2003)

We investigate theoretically the mode-locking properties of an erbium-doped birefringent fiber laser in a unidirectional cavity containing an optical isolator. The mode-locking is achieved through nonlinear polarization rotation. The approach is based on a master equation which takes explicitly into account the angles between the eigen axis of the fiber at each side of the polarizer. The stability conditions of both the stationary and localized solutions are determined. This allows to establish a stability diagram versus the angles which gives the domains where the laser operates in continuous, mode-locked or unstable regime. The model also allows to calculate the pulse duration together with the pulse energy as a function of the orientation of the eigen axis of the fiber with respect to the polarizer.

DOI: 10.1103/PhysRevA.67.013802 PACS number(s): 42.55.Wd

I. INTRODUCTION

Additive pulse mode-locking through nonlinear polarization rotation has been successfully used to obtain stable self-mode-locking in rare-earth doped fiber lasers [1–3]. The experimental configuration consists in a unidirectional ring cavity containing a polarizer placed between two polarization controllers. The basic principle responsible for the mode-locking is the following. The polarization state of a pulse evolves nonlinearly along a birefringent fiber due to the combined effects of self-phase and cross-phase modulation [4] induced on the two orthogonal polarization components, both resulting from optical Kerr effect. A polarization controller is adjusted at the exit of the fiber in such a way that the polarizing isolator lets the central intense part of the pulse pass but blocks the low-intensity pulse wings. Depending on the orientation of the polarization controllers, stable and passive mode-locking can be achieved. This technique of generation of ultrashort pulses can be used either for positive and negative group-velocity dispersion and has been observed using a great variety of rare earth such as erbium, neodymium, or ytterbium. Several theoretical approaches to this problem have been proposed. Among them, we can cite the model developed by Haus and co-workers [5–7] which consists in writing a phenomenological scalar equation assuming that all effects per pass are small. The model takes into account the group-velocity dispersion (GVD), the optical Kerr nonlinearity and a gain medium. It does not include any birefringence of the fiber neither any polarization controller. However, it allows to describe the mode-locking properties of the laser. Its main advantage is that it is relatively simple and a major drawback is that it does not allow to investigate the operating regime of the laser as a function of the position of the polarization controllers. Indeed, different regimes can be experimentally obtained such as continuous, *Q*-switch, mode-lock or unstable [8]. In a recent paper [9], we have proposed a more general model which takes into account the group-velocity dispersion, the optical Kerr nonlinearity, a gain medium, the birefringence of the fiber, and the orientation of the eigen axis of the fiber at each side of the polarizing isolator (θ_+ and θ_-). The configuration studied involves two half-wave plates, instead of polarization controllers (cf. Fig. 1). This particular case is more convenient than the general one because it has only two degrees of freedom (one orientation angle for each phase plate) instead of four. In its final form, the model reduces to a master equation similar to that derived by Haus except that the coefficients explicitly depend on the orientation angles of the eigen axis of the fiber at each side of the polarizer. Our model has been successfully used in the case of a passively mode-locked ytterbium-doped double-clad fiber laser [9]. Indeed, depending on θ_+ and θ_-, the model predicts continuous, mode-lock or unstable operating regime. The resulting theoretical stability diagram is in very good agreement with the experimental one [8]. The ytterbium fiber laser operating around 1.05 μm belongs to the positive group-velocity dispersion case. Since our master equation has given good results in this case, it is of importance to investigate the case of negative group-velocity dispersion.

The aim of this paper is to investigate theoretically the mode-locking properties of an erbium-doped fiber laser operating at 1.55 μm. The mode-locking is achieved through nonlinear polarization rotation in a unidirectional ring cavity containing a polarizer placed between two half-wave plates.

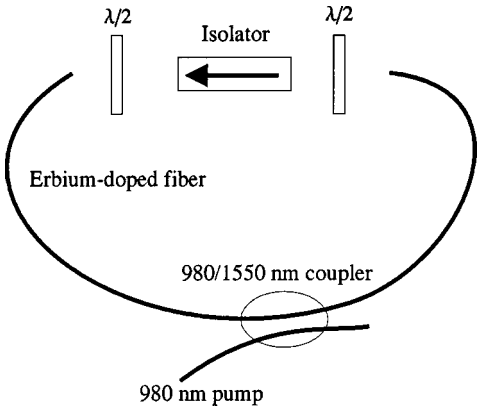

FIG. 1. Schematic representation of the unidirectional ring cavity.

In relation with our previously published work [9], the change of the sign of the chromatic dispersion has strong structural consequences. Indeed, in the present case, the explicit localized solutions of the master equation can be effectively stable. A stability condition has been determined [10]. Therefore, we are able to predict not only the operating mode of the laser, but also the pulse characteristics, which is impossible in the case of positive GVD. The paper is organized as follows. In Sec. II, we briefly report the derivation of the master equation describing the evolution of the amplitude of the electric field for a large number of round trips in the ring cavity. The different regimes of the master equation (stationary solution and short pulse solution) will be examined in Sec. III together with their stability. Results are conveniently summarized in a stability diagram in the plane (θ_+,θ_-) which gives the regions of stable mode-locking, stable continuous operation, and unstable regimes. Sec. IV is devoted to the determination of both the pulse energy and the pulse duration, thus, allowing to optimize the mode-locked laser.

II. THE MASTER EQUATION

The system under study is schematically represented in Fig. 1. It consists of a ring cavity formed by an erbium-doped fiber laser pumped at 980 nm through a multiplexer. The fiber is characterized by the following parameters: length $L=9$ m, GVD $\beta_2=-0.002$ ps^2 m^{-1}, nonlinear coefficient $\gamma=0.002$ W^{-1} m^{-1}, and birefringence $K=0.1$ m^{-1}. A polarizing isolator allows both to obtain a travelling-wave laser and to achieve a mode-lock regime for a suitable orientation of the two half-wave plates which are placed at both sides of the isolator. The phase plates allow to modify the orientation of the eigen axis of the fiber at each side of the polarizer. In the following, we denote by θ_+ and θ_- the angles between the eigen axis of the fiber and the passing axis of the polarizer, respectively, after and before the polarizer.

The starting point of the derivation of the master equation are the equations giving the evolution of the two polarization components in a gain medium with Kerr nonlinearity and GVD. In the framework of the eigen axis of the birefringent fiber moving at the group-velocity, the pulse envelope evolution is described by the following system [3,9,11]:

$$i\partial_z u - Ku - \frac{\beta_2}{2}\partial_t^2 u + \gamma(u|u|^2 + Au|v|^2 + Bv^2u^*) = ig\left(1 + \frac{1}{\omega_g^2}\partial_t^2\right)u, \tag{1}$$

$$i\partial_z v + Kv - \frac{\beta_2}{2}\partial_t^2 v + \gamma(v|v|^2 + Av|u|^2 + Bu^2v^*) = ig\left(1 + \frac{1}{\omega_g^2}\partial_t^2\right)v, \tag{2}$$

where ∂_t denotes the partial derivative operator ∂/∂_t. The parameter β_2 (in ps^2/m) is the GVD coefficient. K (in m^{-1}) is the birefringence parameter and is related to the x and y refractive indexes through the relation $K=\pi(n_x-n_y)/\lambda$, where λ is the optical wavelength. $\gamma=2\pi n_2/(\lambda A_{eff})$ is the nonlinear coefficient, n_2 (in m$^2/W$) is the nonlinear index coefficient, and A_{eff} (in m^2) the effective core area of the fiber. A and B are the dielectric coefficients. In isotropic media, $A=2/3$ and $B=1/3$ [11]. The parameter g is the saturated gain coefficient (in m^{-1}) and ω_g is the spectral gain bandwidth (in ps^{-1}). At first order the gain coefficient is fixed by the fact that it compensates the losses.

We report only the outline of the derivation of the master equation [9]. First, we assume that the GVD β_2, the nonlinear coefficient γ, the gain filtering $\rho=g/\omega_g^2$ are small quantities (of order ε) with respect to the gain g and the birefringence K. This allows to solve the propagation problem using a first-order perturbative approach, as

$$u(z)=u(0)e^{(g-iK)z}+\varepsilon\left[z\left(\rho-\frac{i\beta_2}{2}\right)\partial_t^2u(0) + i\gamma\{u(0)|u(0)|^2+Au(0)|v(0)|^2\}\frac{e^{2gz}-1}{2g} + i\gamma B\tilde{v}(0)^2\tilde{u}(0)^*\frac{e^{(2g+4iK)z}-1}{2g+4iK}\right]e^{(g-iK)z}+O(\varepsilon^2), \tag{3}$$

and an analogous expression for $v(z)$. Just after the polarizer, the field amplitude has a well-defined linear polarization parallel to the polarizing axis

$$\begin{pmatrix} u \\ v \end{pmatrix} = \begin{pmatrix} \cos\theta_+ \\ \sin\theta_+ \end{pmatrix} f_n. \tag{4}$$

We denote, thus, by f_n the amplitude at the beginning of the nth round trip. Then f_{n+1} is computed as a function of f_n using the approximate propagation relations (3), to yield

$$f_{n+1}=\beta e^{gL}\left\{Qf_n+\varepsilon\left[\left(\rho-\frac{i\beta_2}{2}\right)LQ\partial_t^2f_n+iPf_n|f_n|^2\right]\right\} + O(\varepsilon^2), \tag{5}$$

with

$$Q=\cos(\theta_+-\theta_-)\cos KL - i\cos(\theta_++\theta_-)\sin KL, \tag{6}$$

and

$$P=\gamma\left(\frac{e^{2gL}-1}{2g}\left[Q+\frac{A-1}{2}\sin 2\theta_+[\sin(\theta_++\theta_-)\cos KL - i\sin(\theta_+-\theta_-)\sin KL]\right] + \frac{B}{2}\sin 2\theta_+\left[\sin\theta_+\cos\theta_-e^{-iKL}\frac{e^{(2g+4iK)L}-1}{2g+4iK} + \cos\theta_+\sin\theta_-e^{iKL}\frac{e^{(2g-4iK)L}-1}{2g-4iK}\right]\right). \tag{7}$$

β is the transmission coefficient of the polarizer.

The threshold gain value g_0 is determined by the requirement that the amplitude f_n attains some steady state over a large number of round trips, which implies that $|f_{n+1}| = |f_n|$. At leading order ε^0 this gives

$$g_0 = \frac{-1}{2L} \ln(\beta^2[\cos^2(\theta_+ - \theta_-) - \sin 2\theta_+ \sin 2\theta_- \sin^2 KL]). \tag{8}$$

A small excess gain g_1, such that $g = g_0 + \varepsilon g_1$, is allowed. g_1 is still free. Equation (5) then becomes

$$f_{n+1} = e^{i\psi}(1 + \varepsilon g_1 L) f_n + \varepsilon \left(\rho - \frac{i\beta_2}{2} \right) L e^{i\psi} \partial_t^2 f_n + i\varepsilon \frac{P e^{i\psi}}{Q} f_n |f_n|^2 + O(\varepsilon^2), \tag{9}$$

where $e^{i\psi}$ denotes the quantity $\beta e^{g_0 L} Q$, which has a modulus one due to Eq. (8).

Since we are mainly interested in the evolution of the amplitude f_n over a large number of round trips n, it is convenient to approximate the discrete Eq. (9) by a continuous one, to be satisfied by a function f of some continuous variable z, such that $f_n = f(z = nL)$. This equation is

$$i\partial_z f = \frac{-\psi}{L} f + i\varepsilon g_1 f + \varepsilon \left(\frac{\beta_2}{2} + i\rho \right) \partial_t^2 f + \varepsilon \mathcal{D} f |f|^2, \tag{10}$$

where

$$\mathcal{D} = \frac{-P}{QL}. \tag{11}$$

At leading order, the solution of Eq. (10) is

$$f = F e^{i\psi z/L} + O(\varepsilon). \tag{12}$$

The knowledge of the small correction $O(\varepsilon)$ in Eq. (12) on finite propagation distances z is equivalent to the knowledge of the evolution of the leading amplitude F on very large propagation distances $z \propto 1/\varepsilon$. This is proven using the multiscale expansion formalism [12], through the introduction of a slow variable $\zeta = \varepsilon z$. The long-distance evolution of F is

$$i\partial_\zeta F = i g_1 F + \left(\frac{\beta_2}{2} + i\rho \right) \partial_t^2 F + (\mathcal{D}_r + i\mathcal{D}_i) F |F|^2, \tag{13}$$

where $\mathcal{D}_r$ and $\mathcal{D}_i$ are the real and imaginary parts of $\mathcal{D}$. Recall that the "propagation distances" z or ζ represent in fact numbers of round trips. Equation (13) is the cubic complex Ginzburg-Landau (CGL) equation. Notice that Eq. (13) is formally identical to the master equation proposed by Haus *et al.* [7]. However, the coefficients of Eq. (13) explicitly depend on the orientation of the eigen axis of the fiber at both sides of the polarizer. An essential feature is the arising of an effective nonlinear gain or absorption $\mathcal{D}_i$, that results from the combined effects of the nonlinear rotation of the polarization, the losses due to the polarizer, and the linear gain. The value and the sign of $\mathcal{D}_i$ depend on the angles θ_+ and θ_-.

III. SOME EXPLICIT SOLUTIONS OF THE CGL EQUATION

In this section, we are interested in finding some particular solutions of the CGL equation and to study their stability.

A. Stationary solution

The CGL equation admits the following nonzero stationary solution, i.e. with a constant modulus

$$F = \mathcal{A} e^{i(k\zeta - \Omega t)}, \tag{14}$$

where

$$\Omega^2 = \frac{1}{\rho}(\mathcal{D}_i |\mathcal{A}|^2 + g_1) \tag{15}$$

and

$$k = \frac{\beta_2}{2\rho}(\mathcal{D}_i |\mathcal{A}|^2 + g_1) - \mathcal{D}_r |\mathcal{A}|^2. \tag{16}$$

In the particular case $\Omega = 0$, the above solution is a constant. Its amplitude $\mathcal{A}$, assumed to be real for sake of simplicity, and its wave vector k have the determined values

$$\mathcal{A} = \sqrt{\frac{-g_1}{\mathcal{D}_i}} \tag{17}$$

and

$$k = \frac{\mathcal{D}_r}{\mathcal{D}_i} g_1, \tag{18}$$

respectively. Notice that this solution exists only if $\mathcal{D}_i g_1$ is negative.

In Ref. [9], in the case of the ytterbium laser, we have shown that the constant solution is stable when $\mathcal{D}_i < 0$ only. Neither the solution (14) nor the analysis of its stability depend on the sign of the chromatic dispersion. Thus, the above result is valid here. Further, continuous laser emission occurs when the constant solution is stable. The domain of continuous emission coincides, thus, with the regions where $\mathcal{D}_i$ is negative. The sign of $\mathcal{D}_i$ as a function of the angles (θ_+, θ_-) is drawn on Fig. 2. The study has been limited to the region $180° \times 180°$ according to the periodicity of the solution. The hatched domains in Fig. 2 correspond to the negative values of the nonlinear gain $\mathcal{D}_i$. Continuous laser emission occurs in these domains.

B. Localized solutions

In this section, we are interested in solutions of Eq. (13) describing short pulses, which we call localized solutions

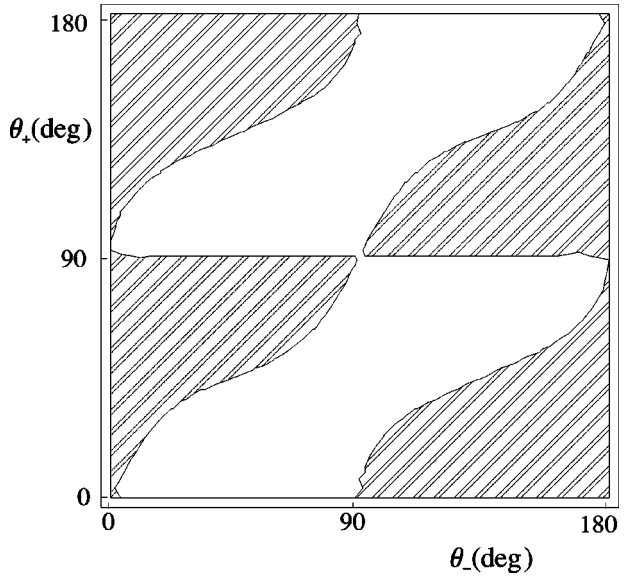

FIG. 2. Stability diagram of the nonzero stationary solution in the plane (θ_+, θ_-). Stability occurs in the hatched zone, and instability in the white domain.

according to the mathematical terminology. In order to use the results of Akhmediev *et al.* [10], we write the CGL Eq. (13) in the normalized form

$$i\partial_\zeta \psi + \frac{1}{2}\partial_\tau^2 \psi + \psi|\psi|^2 = ig_1\psi + iD\psi|\psi|^2 + iR\partial_\tau^2\psi, \quad (19)$$

where $\psi = \sqrt{|\mathcal{D}_r|}F$, $\tau = t/\sqrt{|\beta_2|}$, $R = \rho/|\beta_2|$, and $D = -\mathcal{D}_i/\mathcal{D}_r$. The normalized gain filtering parameter R and the normalized nonlinear gain D are the main parameters of the analysis. They are denoted by β and ε, respectively, in the publications by Akhmediev and his co-workers. Numerical computation shows that $\mathcal{D}_r$ is always negative, so that D and $\mathcal{D}_i$ have the same sign.

Equation (19) admits an explicit localized solution which can be written

$$\psi = a(\tau)^{1+id} e^{-i\omega\zeta}, \quad (20)$$

where

$$d = \frac{3(1+2DR) - \sqrt{9(1+2DR)^2 + 8(D-2R)^2}}{2(D-2R)}, \quad (21)$$

and

$$\omega = \frac{-g_1(1-d^2+4Rd)}{2(d-R+Rd^2)}. \quad (22)$$

d represents the chirp parameter. The amplitude of the pulse writes

$$a(\tau) = MN \,\mathrm{sech}\,(M\tau), \quad (23)$$

where

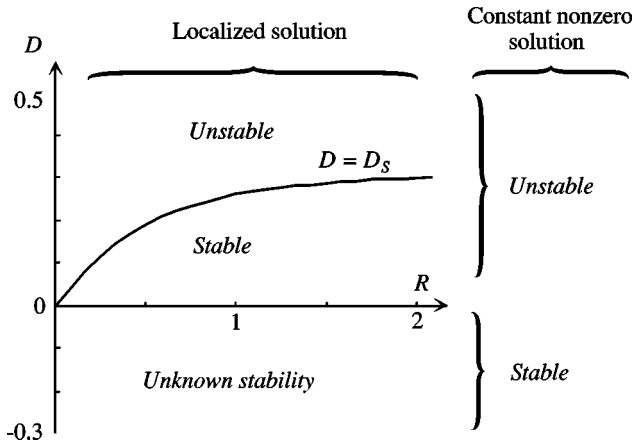

FIG. 3. Diagram showing the stability conditions of the constant nonzero and localized solutions in the plane (R, D).

$$M = \sqrt{\frac{g_1}{d-R+Rd^2}}, \quad (24)$$

and

$$N = \sqrt{\frac{3d(1+4R^2)}{2(2R-D)}}. \quad (25)$$

In the case of positive nonlinear gain D or $\mathcal{D}_i$, the stability of this solution has been studied by Akhmediev *et al.* [10]. They found that the localized solution (20) is stable when the zero solution is unstable, thus, when the linear gain g_1 is positive. Noticing that M is real only if the quantities $(d-R+Rd^2)$ and g_1 have same signs, the stability condition becomes

$$d - R + Rd^2 > 0. \quad (26)$$

This condition can be expressed as follows: in the plane (R, D), the solution is stable below the curve

$$D = D_S = R\frac{3\sqrt{1+4R^2}-1}{4+18R^2}, \quad (27)$$

and unstable above this curve. When the nonlinear gain $\mathcal{D}_i$ or D is negative, no such condition is known at this time. The nonzero constant solution is stable in this case for a positive excess of linear gain g_1, allowing to conclude to continuous laser emission. However, a situation where bistability between continuous and mode-locked emission occurs can be envisaged. This means that the mode-locking will not be self-starting. It will be considered in further study.

C. Discussion

Figure 3 summarizes the stability conditions of the solutions in the plane (R, D). The results are represented in the plane (θ_+, θ_-) in Fig. 4. For this figure, we have taken the values of the parameters given in Sec. II and a spectral gain bandwidth $\omega_g = 15.7\ \mathrm{ps}^{-1}$ corresponding to $\Delta\lambda = 30$ nm [13]. The white regions correspond to stable pulses and then

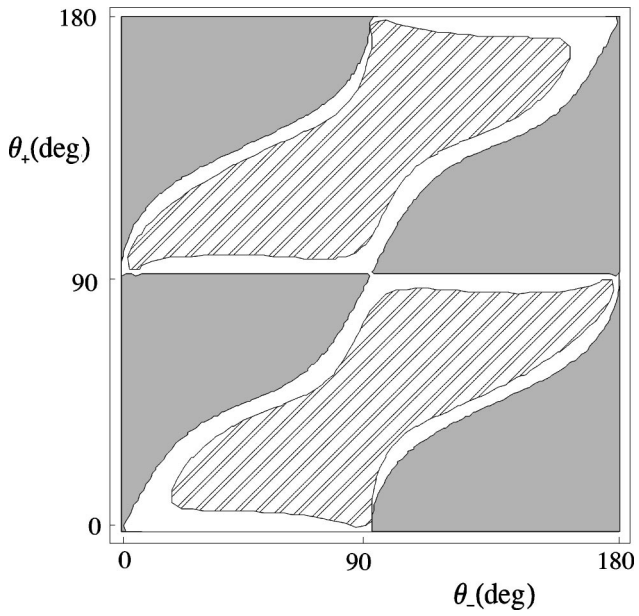

FIG. 4. Stability diagram exhibiting the operating regime of the laser in the plane (θ_+, θ_-). In the gray region, the constant nonzero solution is stable and stability of the mode-locked solution is not known. The white region corresponds to stable mode-locking. In the hatched domain, both solutions are unstable.

to stable self-starting mode-locking because the stationary solution is unstable. In the gray domains the stationary solution is stable and the laser spontaneously operates in cw regime. However, because we do not have information about the stability of the pulses in these regions, the laser also could operate in mode-locking regime if a perturbation is applied. This point deserves further theoretical investigation. Finally, in the hatched regions, both the stationary and the localized solutions are unstable. The laser is expected to operate in chaotic or Q-switch regime.

At this stage, significant differences appear in comparison with the ytterbium laser [8,9]. Especially, the domains of self-starting mode-locking are considerably reduced. In addition, bistability between the continuous and the mode-locked regime is not excluded in the present case, while no bistability was observed in the ytterbium-doped fiber laser.

IV. PULSE CHARACTERISTICS

When the explicit localized solution (20) of the CGL Eq. (13) is stable, it works as an attractor in the sense that any other solution goes close to it after a long enough propagation distance (or number of round trips). Therefore the actual laser pulse is expected to be correctly described in shape and size by Eq. (20).

All quantities in the expression of the pulse are explicitly known, excepted the excess of linear gain g_1. The latter self adjusts to a value yielding a steady state over numerous round trips. This mechanism is determined by the saturation of the gain, which is not taken into account by the model developed above and by the master equation (13). Introducing gain saturation as an external condition allows us to determine completely the characteristics of the pulse.

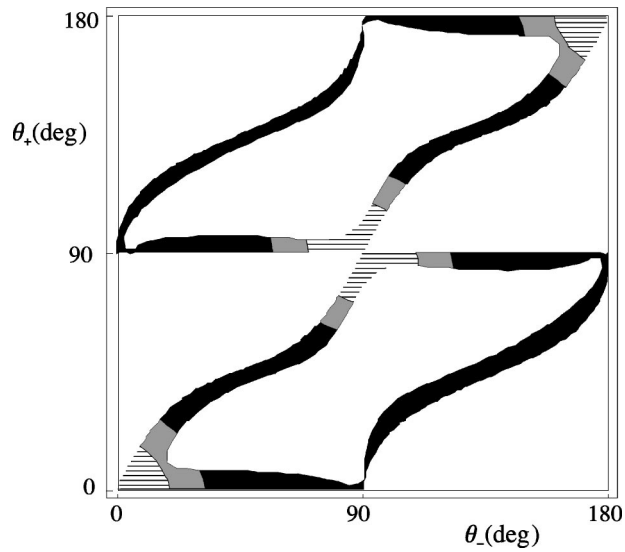

FIG. 5. Evolution of the pulse energy in the plane (θ_+, θ_-). In the hatched region the energy is above 10 pJ, in the gray region the energy is between 5 pJ and 10 pJ and in the black region the energy is below 5 pJ. In the white region, either the pulse are unstable, or their stability is not determined and continuous emission occurs, see Fig. 4.

A. Pulse energy

We first compute the energy as a function of the orientation angles (θ_+, θ_-). At zero order, the saturated gain of the medium is

$$g_0 = \frac{g'}{1 + \dfrac{E}{W_S}}, \tag{28}$$

where g' is the unsaturated gain, W_S the saturation energy, and E the pulse energy. Relation (28) allows to extract the pulse energy provided that the threshold gain value g_0 is known. It has been computed in Sec. II from the fact that the gain must compensate the losses, and is given by relation (8). For the numerical simulations, we take $g' = 1.26\ \mathrm{m}^{-1}$ and $W_S = 0.1$ pJ. The results are presented in Fig. 5 which gives the evolution of E in the plane (θ_+, θ_-). We can notice that the energy strongly varies with θ_+ and θ_-. The most energetic pulses are obtained in the vicinity of $(0°,0°)$ [equivalent to $(180°,180°)$] and $(90°,90°)$. In these regions, the energy is about 10 pJ. This value is very close to the one reported by Haus *et al.* [6]. Our results show that the orientation of the eigen axis of the fiber at each side of the polarizer must be performed carefully because it has a great importance on the resulting energy.

B. Pulse duration

Another important characteristic of a mode-locked laser is the pulse duration. In the configuration investigated in this paper, the pulse duration depends on the angles (θ_+, θ_-). The pulse duration is calculated from relation (23). In normalized units, it writes

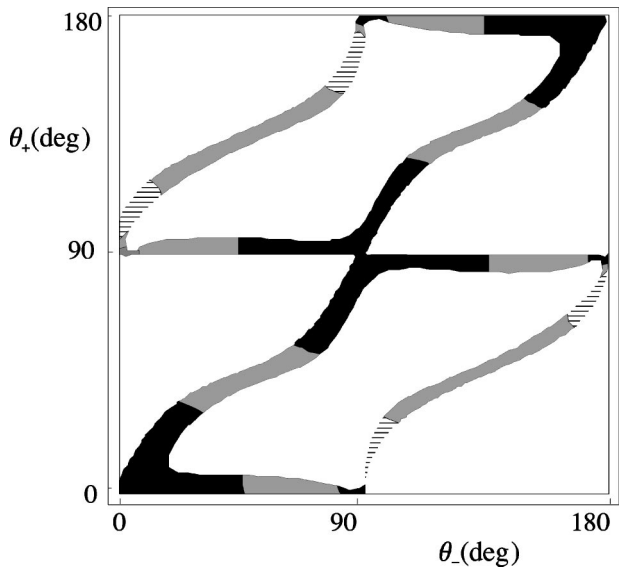

FIG. 6. Evolution of the pulse duration in the plane (θ_+, θ_-). In the hatched region the duration is above 1 ps, in the gray region it is between 0.5 and 1 ps and in the black region below 0.5 ps. The white region has the same meaning as in Fig. 5.

$$\tau_0 = \frac{1}{M}. \tag{29}$$

The expression (24) of M involves the excess gain g_1, which is not known. M can also be found through the computation of the pulse energy $E = \int |F|^2 dt$. Integrating the square modulus of expression (20), we find

$$E = \frac{2\sqrt{|\beta_2|} M N^2}{|\mathcal{D}_r|}. \tag{30}$$

Since the energy E has been obtained using relations (28), and N is explicitly given by Eq. (25), we obtain the expression of the pulse duration t_0 (in ps)

$$t_0 = \tau_0 \sqrt{|\beta_2|} = \frac{2|\beta_2| N^2}{|\mathcal{D}_r| \left(\frac{g'}{g_0} - 1 \right) W_S}, \tag{31}$$

where W_S is in pJ. Fig. 6 shows the evolution of t_0 versus the angles θ_+ and θ_-. Theoretical results show that t_0 undergoes large variations as θ_+ and θ_- vary. Only small regions lead to ultrashort pulses. This is due to the fact that for these values of the angles the top of the pulse undergoes lower losses than the wings. The shortest pulse width predicted by our model is about 90 fs. This lowest value depends on fiber characteristics. In particular, the spectral gain bandwidth takes a prominent part because it can directly limit the pulse duration. Beyond $\Delta\lambda \simeq 15$ nm, the pulse duration does not change when $\Delta\lambda$ is varied. In this case, the limitation is due to the GVD. Below $\Delta\lambda \simeq 15$ nm, the pulse width increases when $\Delta\lambda$ decreases. The pulse duration is then limited by the spectral gain bandwidth. In addition, we can notice that the shortest pulses are obtained for the same values of the angles θ_+ and θ_- which maximize the pulse energy. This result is important because it means that both parameters (duration and energy) can be optimized simultaneously.

V. CONCLUSION

We have derived a master equation that describes the mode-locking properties of an erbium-doped birefringent fiber laser in a unidirectional cavity containing an optical isolator. The master equation is of CGL type, its coefficients depend explicitly on the angles between the eigen axis of the fiber at each side of the polarizer. Indeed, the mode-locking is achieved through nonlinear polarization rotation, which is taken into account in the model. The dependency of the laser properties with regard to the angles is, thus, explicitly taken into account by the master equation.

The CGL equations admits several explicit solutions, among which two are of interest here: the nonzero constant solution and the localized one. Using the known stability conditions of these solutions, we have been able to predict the operating mode of the laser as a function of the angles. This yields a stability diagram versus the angles which gives the domains where the laser operates in continuous, mode-locked or unstable regime.

Furthermore, the explicit localized solution is expected to describe the actual laser pulse. When gain saturation is taken into account, the model therefore allows to compute the pulse characteristics, especially its duration and its energy. The results are given as functions of the orientation of the eigen axis of the fiber with respect to the polarizer. A maximum energy of about 10 pJ, with a minimum duration of about 90 fs have been obtained. The domains of the angular parameters for which mode-locking occurs are small. The regions of maximum energy in these domains coincide with the regions of minimum pulse duration. Optimization is obtained this way in two small regions in each 180×180 degrees period of the angular parameters.

Additional theoretical work is needed to fully characterize the stability of the pulses when the nonlinear gain is negative.

[1] L.E. Nelson, D.J. Jones, K. Tamura, H.A. Haus, and E.P. Ippen, Appl. Phys. B: Lasers Opt. **65**, 277 (1997).
[2] H.A. Haus, E.P. Ippen, and K. Tamura, IEEE J. Quantum Electron. **30**, 200 (1994).
[3] A.D. Kim, J.N. Kutz, and D.J. Muraki, IEEE J. Quantum Electron. **36**, 465 (2000).
[4] M. Hofer, M.E. Fermann, F. Haberl, M.H. Ober, and A.J. Schmidt, Opt. Lett. **16**, 502 (1991).
[5] K. Tamura, H.A. Haus, and E.P. Ippen, Electron. Lett. **28**, 2226 (1992).
[6] H.A. Haus, K. Tamura, L.E. Nelson, and E.P. Ippen, IEEE J. Quantum Electron. **31**, 591 (1995).

[7] H.A. Haus, J.G. Fujimoto, and E.P. Ippen, J. Opt. Soc. Am. B **8**, 2068 (1991).

[8] Ammar hideur, Thierry Chartier, Marc Brunel, Mohamed Salhi, Cafer Özkul, and François Sanchez, Opt. Commun. **198**, 141 (2001).

[9] H. Leblond, M. Salhi, A. Hideur, T. Chartier, M. Brunel, and F. Sanchez, Phys. Rev. A **65**, 063811 (2002).

[10] N.N. Akhmediev and A. Ankiewicz, *Solitons, Nonlinear Pulses and Beams* (Chapman and Hall, London, 1997); N.N. Akhmediev and V.V. Afanasjev, Phys. Rev. Lett. **75**, 2320 (1995).

[11] G.P. Agrawal, *Nonlinear Fiber Optics*, 2nd ed. (Academic Press, New York, 1995).

[12] T. Taniuti and C.-C. Wei, J. Phys. Soc. Jpn. **24**, 941 (1968); T. Taniuti and N. Yajima, J. Math. Phys. (Cambridge, Mass.) **14**, 1389 (1973).

[13] *Rare-Earth Doped Fiber Lasers and Amplifiers*, edited by M.J.F. Digonnet (Dekker, New York, 1993).